A COAXIAL LINE FILLED WITH TWO NON-CONCENTRIC DIELECTRICS*

D. J. Angelakos
University of California
Berkeley, California

Summary

An analysis has been made of a coaxial transmission line composed of two coaxial cylindrical conductors. Two dielectrics fill different angular portions of the volume between the conductors. The propagation constants (primarily the guide wavelength) are determined by a resonant condition applied to the plane transverse to the direction of propagation. Experimental verification is given for near unity values of the ratio of the outer to the inner radius. In addition, an experimental investigation has been made of the properties of the guide wavelength as a function of frequency and larger ratios of the radii.

* * * * * * * * * * * *

I. Introduction

The propagation constants of coaxial transmission lines with coaxial dielectric cylinders have been determined by means of several methods. The problem has been treated as a boundary value problem as well as a modal problem.[1,2]

On the other hand, the composite structure of coaxial cylinders and a wedge-shaped dielectric material does not lend itself to a simple analysis by means of the solution of Maxwell's Equations subject to the proper boundary conditions. A simple approach which yields good results is made here using an approximate modal method.

II. Theory and Experimental Results

The waveguide shown in Fig. 1(a) consists of two uniform coaxial cylindrical conductors, the space between the cylinders being partially filled with material of dielectric constant ε_2. The remaining volume has a dielectric constant ε_1. The structure has even symmetry about the plane AA' and through the use of the bisection theorem, can be considered as a "bent" waveguide of width λ_g and length $2\pi\rho$ where ρ is an average radius. The ends of the "bent" waveguide are open circuited. The requirement that the total admittance looking in both directions at the point T yields the resonant frequencies can be written as follows:[3]

$$Y_{02} \tan \left[\frac{2\pi}{\lambda_{c_2}} \phi \rho \right] + Y_{01} \tan \left[\frac{2\pi}{\lambda_{c_1}} (\pi - \phi) \rho \right] = 0.$$

---

* This work was done at the Electronics Research Laboratory of the University of California and was supported in part by the U.S. Office of Naval Research.

Y_{02} and Y_{01} are the characteristic admittances of the sections 2 and 1 respectively. The wavelengths λ_{c2} and λ_{c1} are the wavelengths of propagation of the fields into region 2 and region 1 respectively of the "bent" waveguide. The angle is shown in Fig. 1(b).

For the region 1,

$$Y_{01} = \frac{k_{c_1}}{\omega\mu} = \left[\left(\frac{2\pi}{\lambda_0} \right)^2 \epsilon_2 - \left(\frac{2\pi}{\lambda_g} \right)^2 \right]^{\frac{1}{2}} \Big/ \omega\mu$$

and

$$\frac{2\pi}{\lambda_{c_1}} = \left[\left(\frac{2\pi}{\lambda_0} \right)^2 \epsilon_1 - \left(\frac{2\pi}{\lambda_g} \right)^2 \right]^{\frac{1}{2}}$$

Similarly, for region 2,

$$Y_{02} = \frac{k_{c_2}}{\omega\mu} = \left[\left(\frac{2\pi}{\lambda_0} \right)^2 \epsilon_2 - \left(\frac{2\pi}{\lambda_g} \right)^2 \right]^{\frac{1}{2}} \Big/ \omega\mu$$

and

$$\frac{2\pi}{\lambda_{c_2}} = \left[\left(\frac{2\pi}{\lambda_0} \right)^2 \epsilon_2 - \left(\frac{2\pi}{\lambda_g} \right)^2 \right]^{\frac{1}{2}}$$

For both, λ_0 is the free-space wavelength, λ_g is the unknown resonant wavelength or propagation wavelength in the axial direction of Fig. 1(c). Since $\lambda_1 = \frac{\lambda_0}{\sqrt{\epsilon_2}}$, the above relations may be arranged in the following form:

$$Y_{02} \Big/ Y_{01} = \left[\frac{\epsilon_2 - \left(\frac{\lambda_0}{\lambda_g} \right)^2}{\epsilon_1 - \left(\frac{\lambda_0}{\lambda_g} \right)^2} \right]^{\frac{1}{2}} = \frac{1}{j} \left[\frac{\frac{\epsilon_2}{\epsilon_1} - \left(\frac{\lambda_1}{\lambda_g} \right)^2}{\left(\frac{\lambda_1}{\lambda_g} \right)^2 - 1} \right]^{\frac{1}{2}}$$

and

$$\frac{2\pi}{\lambda_{c1}} = j \frac{2\pi}{\lambda_1} \left[\left(\frac{\lambda_1}{\lambda_g} \right)^2 - 1 \right]^{\frac{1}{2}}, \quad \frac{2\pi}{\lambda_{c2}} = \frac{2\pi}{\lambda_1} \left[\frac{\epsilon_2}{\epsilon_1} - \left(\frac{\lambda_1}{\lambda_g} \right)^2 \right]^{\frac{1}{2}}.$$

Hence, the resonant condition becomes:

(1)

$$\tanh \left[\frac{2\pi}{\lambda_1} \sqrt{\left(\frac{\lambda_1}{\lambda_g} \right)^2 - 1} \left(\pi - \phi \right) \rho \right] = \sqrt{\frac{\frac{\epsilon_2}{\epsilon_1} - \left(\frac{\lambda_1}{\lambda_g} \right)^2}{\left(\frac{\lambda_1}{\lambda_g} \right)^2 - 1}} \tan \left[\frac{2\pi}{\lambda_1} \sqrt{\frac{\epsilon_2}{\epsilon_1} - \left(\frac{\lambda_1}{\lambda_g} \right)^2} \, \phi\rho \right].$$

If the arguments are small,

$$\frac{2\pi}{\lambda_1}\sqrt{\left(\frac{\lambda_1}{\lambda_g}\right)^2 - 1}\;(\pi - \phi)\rho = \sqrt{\frac{\frac{\epsilon_2}{\epsilon_1} - \left(\frac{\lambda_1}{\lambda_g}\right)^2}{\left(\frac{\lambda_1}{\lambda_g}\right)^2 - 1}} \cdot \frac{2\pi}{\lambda_1}\sqrt{\frac{\epsilon_2}{\epsilon_1} - \left(\frac{\lambda_1}{\lambda_g}\right)^2}\,\phi\rho .$$

The ratio of $\frac{\lambda_g}{\lambda_1}$ then becomes independent of the average radius ρ and

$$\frac{\lambda_g}{\lambda_1} = \frac{1}{\sqrt{\frac{\phi}{\pi}\left(\frac{\epsilon_2}{\epsilon_1} - 1\right) + 1}} \tag{2}$$

Equation (2) can be obtained from the consideration of the "static" problem in the diagram of Fig. 2.

The capacitances per unit length of the regions 1 and 2 are:

$$C_1 = \frac{2\epsilon_1 (\pi - \phi)}{\ell n\, b/a} \quad \text{and} \quad C_2 = \frac{2\epsilon_2 \phi}{\ell n\, b/a} \quad \text{respectively.}$$

The total equivalent capacitance is:

$$C_e = C_1 + C_2 = C_{01}\left[\frac{\phi}{\pi}\left(\frac{\epsilon_2}{\epsilon_1} - 1\right) + 1\right]$$

where $$C_{01} = \frac{2\pi\epsilon_1}{\ell n\, b/a} .$$

The equivalent phase velocity, V_e, and wavelength of propagation, λ_g are:

$$V_e = \frac{1}{\sqrt{LC_e}} = f\lambda_g = \frac{f\lambda_1}{\sqrt{\frac{\phi}{\pi}\left(\frac{\epsilon_2}{\epsilon_1} - 1\right) + 1}}$$

and so

$$\frac{\lambda_g}{\lambda_1} = \frac{1}{\sqrt{\frac{\phi}{\pi}\left(\frac{\epsilon_2}{\epsilon_1} - 1\right) + 1}}$$

The variation of the propagation wavelength as a function of the amount of filling by the dielectric as calculated from the "static" formula (2) is shown in Fig. 3. The experimental points are for a considerable number of frequencies and for a ratio of the radii: $\frac{b}{a} = 1.6$. These points for most of the frequency range lie within the circles shown. A detailed investigation of the deviation of the ratio of $\frac{\lambda_g}{\lambda_1}$, as calculated from resonant condition (1), from the static approximation of (2) as a function of the frequency is summarized in Fig. 4.

For this set of data, the relative dielectric constant of region 1 is 1.0 (air) and that of region 2 is 2.8 (Hysol plastic). The ratio $\frac{b}{a}$ is 1.60. (Actual dimensions: b = 1/2", a = 5/16", frequency range between 1,000 mcps and 3,500 mcps.)

The effect of the variation of the ratio $\frac{b}{a}$ on the wavelength has been investigated for a large frequency range. Fig. 5 indicates this variation for several frequencies. As the ratio of b to a becomes larger, the "bent" waveguide approximation becomes worse.[4]

In the limit of $\frac{b}{a} \to \infty$, the physical shape of the dielectric approaches a dielectric wedge. Fig. 6 illustrates that the ratio $\frac{\lambda_g}{\lambda_1}$ variation with frequency is small. The deviation from the static approximation due to the waveguide property is compensated in part by a correction necessitated by the circular bend.

The modal structure of the fields within this partially filled coaxial line was examined in detail. The guide wavelength was measured for the three positions indicated in Fig. 7. Within experimental accuracy, the guide wavelength, the position of voltage minima and voltage maxima remained unchanged for the three positions. This was true for a large number of frequencies and for two conditions of load; e.g. (1) short circuit and (2) arbitrary resistive load.

By rotating the inner structure of the coaxial cable dielectric assembly, the charge distribution on the inner surface of the outer conductor was obtained. As is seen in Fig. 8, the charge distribution does follow a cosinusoidal type of variation from the plane of symmetry in region 2 and hyperbolic cosine variation in region 1; it is rapidly changing about the plane of the dielectric discontinuity. The ratio of charge densities of the two regions is equal to the ratio of the dielectrics used. (Hysol plastic, $\frac{\epsilon_2}{\epsilon_1} = 2.8$.) The frequency for this measurement was 2000 mcps.

The coaxial line in which all the measurements were made consists of a slotted outer conductor of 1 inch inner radius. The dielectric used was a low-loss Hysol plastic of a relative dielectric constant of 2.8. The slot through which the search probe was inserted was covered by a sliding shield so that slot mode excitation was negligible.

Conclusion

The partially filled coaxial cable can be analyzed to a very good approximation by a simple static method as long as the ratio of the outer to the inner radius is small. Even for frequencies high enough to almost propagate the next higher mode, this approximate method is useful. The method could be extended to similar problems which do not lend themselves to easy solution by means of exact boundary value problem methods. The dielectric wedge obtained as a consequence of a large ratio of the outer to the inner radius produces a guide wavelength near to that calculated approximately.

References

(1) Beam and Dobson, "Proc. of National Electronics Conference," pp. 301-311; 1952.

(2) Marcuvitz, "Waveguide Handbook," (Book) McGraw-Hill Book Company, Inc., New York, pp. 396-397.

(3) Marcuvitz, "Waveguide Handbook," (Book) McGraw-Hill Book Company, Inc., New York, pp. 387-388.

(4) Marcuvitz, "Waveguide Handbook," (Book) McGraw-Hill Book Company, Inc., New York, pp. 333.

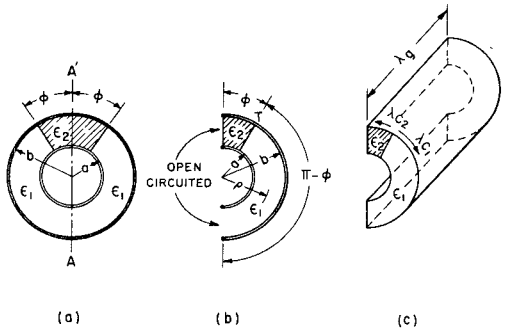

Fig. 1 - Details of the coaxial line considered as a bent waveguide.

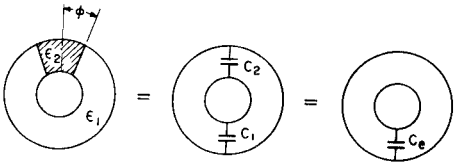

Fig. 2 - Static or low-frequency consideration of the partially filled coaxial line.

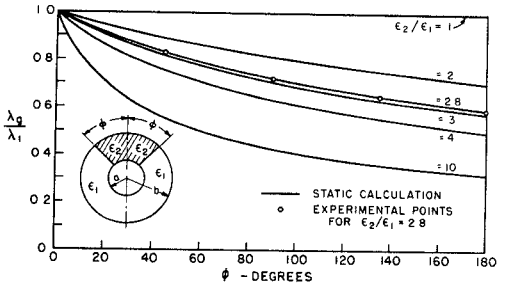

Fig. 3 - Low-frequency approximate guide-wavelength variation as a function of angular dielectric filling.

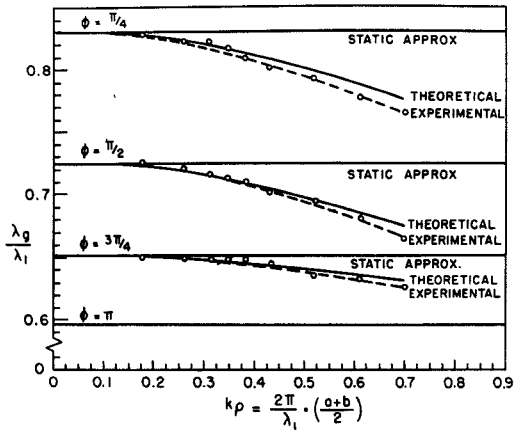

Fig. 4 - Comparison of the approximate method, modal method and experimental results as a function of frequency. ($\epsilon_2/\epsilon_1 = 2.8$; $b/a = 1.6$.)

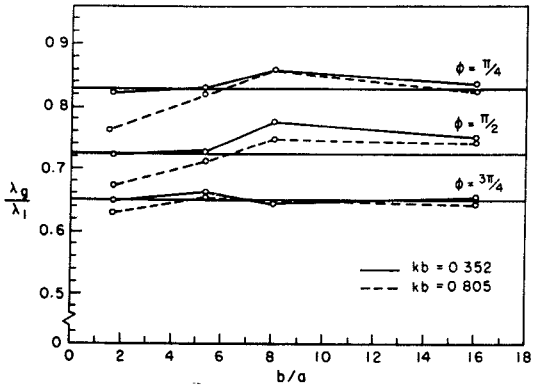

Fig. 5 - The effect of the ratio of radii on the wavelength in the guide.

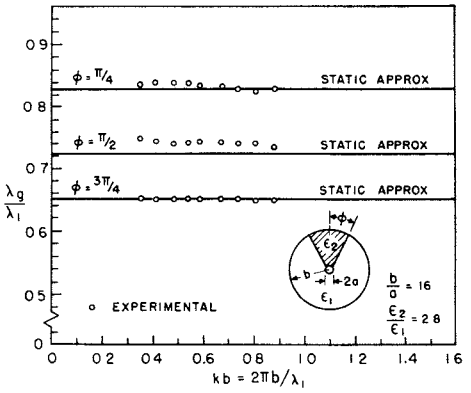

Fig. 6 - Variation of the guide-wavelength as a function of frequency for a large ratio of the radii.

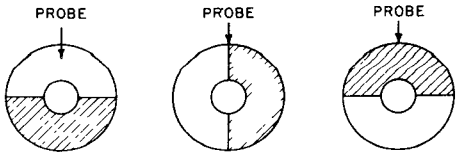

Fig. 7 - Positions of the search probe in the composite line.

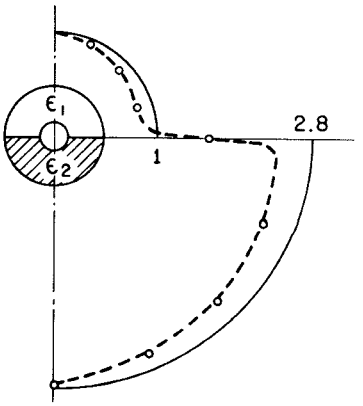

Fig. 8 - Charge-density distribution on the inner surface of the outer conductor for a partially filled coaxial line.